SIMULATION OF MULTISTAGE HYDROGEN COMPRESSION FOR DIFFERENT DISCHARGE PRESSURES WITH WASTE HEAT RECOVERY BASED ON ORC TECHNOLOGY

Alexandra Pavlidi[1], Konstantinos Braimakis[2], Sotiris Karellas[3] and George Tsatsaronis[4]

[1] Centre on Sustainable Energy, INRASTES, National Centre for Scientific Research "Demokritos", Athens, Greece, a.pavlidi@ipta.demokritos.gr, CA
[2] Laboratory of Refrigeration, Air Conditioning and Solar Energy, School of Mechanical Engineering, National Technical University of Athens, Greece, mpraim@central.ntua.gr
[3] Laboratory of Steam Boilers and Thermal Plants, School of Mechanical Engineering, National Technical University of Athens, Greece, sotokar@mail.ntua.gr
[4]Centre on Sustainable Energy, INRASTES, National Centre for Scientific Research "Demokritos", Athens, Greece, and Institute for Energy Engineering, Technical University of Berlin, Germany, georgios.tsatsaronis@tu-berlin.de

Abstract:

The increasing demand for hydrogen as a low-carbon energy carrier highlights the importance of efficient compression technologies, particularly for high-pressure-storage and transport applications. This study investigates multistage mechanical hydrogen compression systems designed for final discharge pressures of 350 bar and 700 bar, coupled with waste heat recovery using an Organic Rankine Cycle (ORC). A steady-state simulation model is developed in Aspen Plus to evaluate system performance, including compressor operation, intercooling requirements, and thermal energy recovery potential. The compression systems are optimized with respect to interstage pressure ratios to minimize total compression work while respecting the operational constraint of maximum discharge temperature. The thermal energy rejected in the intercoolers is recovered and utilized as the heat source for the ORC, which is modeled to assess its capability for electricity generation. Key performance indicators include specific compression work, intercooler heat duty, ORC power output, and overall electricity savings. The results indicate that higher discharge pressures lead to increased compression work, while optimized staging maintains pressure ratios within acceptable operational limits. The four-stage configuration exhibits higher waste heat recovery potential compared to the five-stage system due to higher temperature levels in the intercooler streams. The integration of the ORC system results in very modest electricity savings, ranging from 1.4–2% for the four-stage system and 0.98–1.5% for the five-stage system. Overall, the study demonstrates that while waste heat recovery from hydrogen compression is technically feasible, its effectiveness is strongly dependent on the temperature level of the available heat. The findings provide useful insights into the thermodynamic integration of compression and recovery systems, supporting the design of more energy-efficient hydrogen infrastructure.

Keywords:

Hydrogen mechanical compression, Modeling and simulation, Organic Rankine Cycle, Waste heat recovery

1. Introduction

Driven by European Union regulations targeting greenhouse gas emission reductions and deep decarbonization of the industrial sector [1], a significant transition toward alternative fuels is currently underway. Among these, hydrogen is emerging as a promising energy carrier, as it offers a low-carbon pathway with zero direct CO_2 emissions at the point of use, high gravimetric energy density, fuel flexibility across multiple sectors, and strong potential for integration with renewable energy systems through green hydrogen production pathways [2]. However hydrogen exhibits the lowest volumetric density among the most commonly used fuels, which creates substantial challenges for storage and transportation. At ambient conditions hydrogen has a volumetric energy density of approximately 0.01 MJ/l, compared to about 35-38 MJ/l for gasoline, 22-24 MJ/l for Liquified Natural Gas, and 9-10 MJ/l for Compressed Natural Gas at 250 bar. Even when compressed to high pressures (700 bar), hydrogen reaches roughly 5-6 MJ/l, which remains significantly lower than that of

liquid hydrocarbons [3]. Consequently, high-pressure compression or liquefaction is typically required to enable practical hydrogen storage and transport over long distances. In recent years, hydrogen compression technologies continue to evolve, while various projects highlight the novelties of various compression methods. The COSMHYC series of projects [4] focuses on the coupling of mechanical and metal hydride compression technologies, H2REF [5] is using bladder accumulation-based compressors as an alternative to the commonly utilized compressor types, while various other projects like ELCHPEM2.0 [6] focus on electrochemical compression. Mechanical compression systems generate substantial interstage waste heat, which can potentially be recovered and used in a thermal cycle for electricity generation. Reference [7] developed an integrated thermoelectric generator-hydrogen compression system for hydrogen storage and waste heat recovery (TEG-CHSWHR), with particular emphasis on the influence of inlet conditions on system performance and energy recovery efficiency. Nevertheless, studies that explicitly investigate waste heat recovery from hydrogen compression processes remain limited in the available literature. The present study addresses this gap by developing a green hydrogen compression system coupled with an Organic Rankine Cycle (ORC) for the effective conversion of compression-stage waste heat into electrical power.

2. Methodology

2.1. System description

In this study, a multistage mechanical hydrogen compression system was designed. To address the requirements of different downstream applications with distinct discharge pressure levels, two separate simulation scenarios were developed, targeting final compression pressures of 350 bar and 700 bar. A discharge pressure of 350 bar is typically associated with applications such as hydrogen refueling for heavy-duty vehicles (e.g., buses and trucks) and tube trailer storage, commonly employing Type I and Type II pressure vessels. In contrast, a discharge pressure of 700 bar is primarily required for light-duty fuel cell vehicles, where higher storage density is necessary, and is typically associated with advanced composite storage systems such as Type III and Type IV tanks [8-10]. Every system consists of compressors, intercoolers and dry coolers for the recirculation of the cooling water. In addition, a waste heat recovery configuration based on an ORC was investigated to evaluate the potential for electricity generation from compression-stage heat rejection. The four-stage system flowsheet is depicted in Figure 1, while the five-stage system flowsheet in Figure 2.

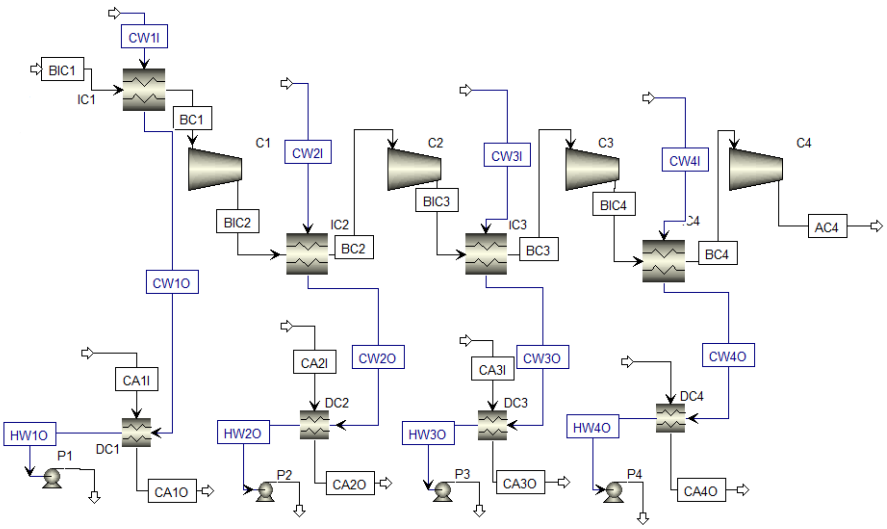

Figure 1. *Aspen Plus flowsheet of the four-stage compression system*

The hydrogen stream is assumed to be produced via water electrolysis in an electrolyzer powered by renewable electricity (green hydrogen). The electrolyzer is rated at 100 MW, with a higher heating value (HHV) efficiency of 80%. Hydrogen exits the electrolyzer and enters the compression system at a mass flow rate of 1780 kg/h, temperature of 60 °C and pressure of 20 bar.

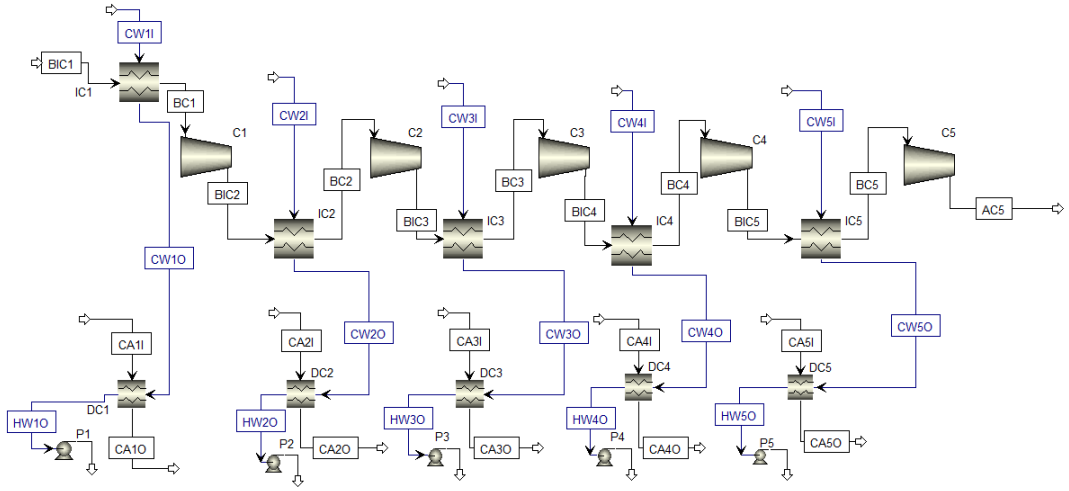

Figure 2. *Aspen Plus flowsheet of the five-stage compression system*

Prior to each compression stage the hydrogen is cooled in the intercoolers to a target temperature of 38 °C. Interstage cooling is required to ensure that the compressor discharge temperature does not exceed the recommended limit of 150 °C, thereby preventing potential damage to sealing components [11]. Cooling is provided by pressurized water at 5 bar and 30 °C, which absorbs heat from the hydrogen stream and rejects it through dry coolers in the base-case configuration. The dry coolers operate with atmospheric air (at 20 °C and 1 atm) and a fan motor efficiency of 90% and an associated pressure drop of 0.0015 bar [12], restoring the cooling water temperature to 30 °C. The compression units are assumed to be reciprocating compressors with an isentropic efficiency of 80%, consistent with large-capacity hydrogen compression systems [13]. For reciprocating compressors operating above 70 bar the allowable pressure ratio per stage is typically limited to the range of 2-2.5 [14], accordingly four compression stages are implemented for delivery at 350 bar and five stages for delivery at 700 bar. Table 1 includes the most important system assumptions, constraints and initial conditions.

Table 1. *System inlets, assumptions and parameters*

Hydrogen inlet conditions	
Mass flow rate	1780 kg/h
Temperature	60 °C [15]
Pressure	20 bar [16]
Intercoolers operation	
Water inlet temperature	30 °C
Hydrogen outlet temperature	38 °C
Water outlet temperature	$T_{H_2,in}$-10
Dry coolers operation	
Air inlet temperature	20 °C
Air outlet temperature	40 °C
Water outlet temperature	30 °C
Fan motor efficiency	90% [12]
Air pressure drop	0.0015 bar [12]

For waste heat recovery, a standard ORC configuration is employed, featuring a pump, evaporator, expander, and air-cooled condenser (ACC). The process begins as the pump pressurizes the working fluid, which is subsequently vaporized by the Heat Transfer Fluid (HTF) within the evaporator. The water streams exiting the intercoolers are mixed to form the HTF entering the evaporator. The high-pressure vapor of the working fluid exiting the evaporator drives the expander to generate mechanical power, which a generator then converts into electricity. After expansion, the fluid is cooled in the ACC until it reaches a subcooled liquid state, completing the cycle as it returns to the pump. The HTF, upon exiting the evaporator, remains at a higher

temperature than the required 30°C intercooler inlet temperature. Therefore, it undergoes further cooling in the HTFC to reach this temperature.

2.2. Process modeling

The steady-state simulation of the multi-stage compression system as well as the ORC configuration is implemented with the Aspen Plus software [17], using basic material streams, built-in blocks and design specification blocks. Aspen Plus' model analysis tools are also used for the optimization and sensitivity analysis of parameters of the system.

2.2.1. Compression system

The hydrogen compression stages are simulated using the standard Compressor block available in Aspen Plus. The compressor model is configured under isentropic operation with an assumed isentropic efficiency of 80% [13] and a mechanical efficiency of 98% [13]. For each compression stage the outlet condition is specified in terms of discharge pressure, determined based on the optimal per-stage pressure ratio, calculated using Equation (1).

$$p_{ratio} = \left(\frac{p_{final}}{p_{initial}}\right)^{\frac{1}{N}} \quad (1)$$

where $p_{initial}$ is the pressure of the hydrogen at the inlet of the compression system (20 bar), p_{final} is the final discharge pressure (equal to 350 bar for the four-stage system and to 700 bar for the five-stage system) and N is the number of stages. This value serves both to define the necessary outlet pressure specification within the Aspen Plus compressor model and to provide a physically meaningful initial estimate that enhances the convergence and robustness of the optimization procedure.

The compressors' electric power consumption is calculated through Equation (2).

$$P_{e,c} = \dot{m}_{H_2} \frac{h_{H_{2,out}} - h_{H_2.in}}{\eta_m} \quad (2)$$

where $P_{e,c}$ is the compressor's electric power consumption, $\dot{m}_{H_2}$ is the hydrogen mass flow rate, $h_{H_{2,i}}$ is the hydrogen's enthalpy at the outlet and inlet of the compressor and η_m is the mechanical efficiency.

The built-in optimization tool is enabled to ensure efficient compressor operation. The objective function is defined as the minimization of the total compression work, achieved by varying the discharge pressures of the first N-1 compression stages. To account for operational and mechanical limitations, constraints are imposed to maintain the discharge temperature of each compressor below 150 °C [11], thereby mitigating the risk of excessive thermal stress and equipment wear.

The intercoolers are modeled using the MHeatX block. The hydrogen outlet temperature is specified at 38 °C for each stage. The operation of each intercooler is coupled with a Design-Spec block that adjusts the cooling water mass flow rate to maintain its outlet temperature 10 °C below the hydrogen inlet temperature to the intercooler. This approach enables effective heat removal while preserving a realistic temperature driving force across the heat exchanger. Moreover it maximizes the recoverable thermal energy available for utilization in the ORC-based waste heat recovery configuration. The heat duty of the intercoolers is calculated by Equation (3).

$$Q = \dot{m}_{H_2O} \times \left(h_{H_2O,out} - h_{H_2O,in}\right) = \dot{m}_{H_2} \times \left(h_{H_2,in} - h_{H_2,out}\right) \quad (3)$$

where Q is the heat duty of the intercoolers, $\dot{m}_i$ is the mass flow rate of the *ith* component and $h_{i,j}$ is the specific enthalpy of the *ith* component at the inlets and outlets of the intercooler respectively. The specific heat duty is calculated using Equation (4) and is defined as the heat duty of each intercooler normalized by the hydrogen mass flow rate.

$$q = \frac{Q}{\dot{m}_{H_2}} \quad (4)$$

The dry coolers are modeled following an approach similar to that adapted for the intercoolers. The MHeatX block is employed, with the air outlet temperature specified at 40 °C. Each dry cooler is coupled with a Design-Spec block that regulates the air mass flow rate to ensure that the cooling water outlet temperature is maintained at 30 °C. The power consumption of the dry-coolers fans is calculated by Equation (5).

$$P_{e,DC} = \dot{V}_{air} \times \frac{\Delta P_{air}}{\eta_{motor}} \tag{5}$$

where $\dot{V}_{air}$ is the volumetric flow rate of the air in m^3/s, ΔP_{air} is the pressure drop in Pa and η_{motor} is the motor efficiency. The combined operation of the intercoolers and dry coolers represents the complete cooling system configuration within the overall process simulation. And consequently the total electric power consumption of the system is equal to the sum of the consumption of all compression stages plus the consumption of the dry-coolers fans.

The validation of the compression model is conducted against literature data reported in [18], by varying the system discharge pressure and evaluating the corresponding compression losses expressed as a fraction of the hydrogen lower heating value (LHV). The results are presented in Figure 3.

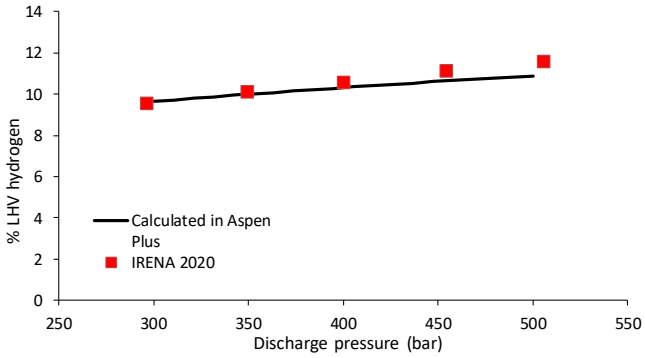

Figure 3. *Comparison of the hydrogen LHV% compression losses for compression at various discharge pressures of the present model with literature data [18]*

A constant 4% LHV penalty is incorporated into all simulation results to account for compression losses associated with the electrolysis stage and the initial pressure increase to 20 bar. For lower pressures, the simulation results follow the literature data with adequate accuracy, while for higher values a larger deviation is observed.

2.2.2. Organic Rankine Cycle

The waste heat recovery ORC is modeled under steady-state conditions using the Peng–Robinson equation of state with the Boston–Mathias alpha function as the thermodynamic property method [19], in line with previous work by the authors [20-23]. Pressure drops and heat losses in piping and system components are neglected. The evaporator and condenser are modeled as countercurrent heat exchangers, while the pump and expander are represented assuming fixed efficiencies, namely the pump efficiency $\boldsymbol{\eta_{pump}}$ and the expander isentropic efficiency $\boldsymbol{\eta_{is,exp}}$.

The net electrical power output of the ORC, $\boldsymbol{P_{e,ORC}}$, is defined as the difference between the gross power produced by the expander-generator and the auxiliary power consumptions of the pump and the air-cooled condenser (ACC) fan (Equation (6)):

$$P_{e,ORC} = P_{e,exp} - P_{e,pump} - P_{e,ACC,fan} \tag{6}$$

The electrical power generated by the expander is calculated based on the working fluid mass flow rate $\dot{m}_{wf}$, the enthalpy drop across the expander $h_{exp,in} - h_{exp,out}$, the electromechanical efficiency $\eta_{em,exp}$, and the isentropic efficiency $\eta_{is,exp}$, as shown in Equation (7).

$$P_{e,exp} = \eta_{em,exp} \times \dot{m}_{wf} \times \left(h_{exp,in} - h_{exp,out}\right) = \eta_{em,exp} \times \eta_{is,exp} \times \dot{m}_{wf} \times \left(h_{exp,in} - h_{exp,out,is}\right) \tag{7}$$

The pump power consumption is determined from the working fluid mass flow rate, the enthalpy rise across the pump and the pump efficiencies (Equation (8)).

$$P_{e,pump} = \dot{m}_{wf} \frac{(h_{pump,out} - h_{pump,in})}{\eta_{pump}} = \dot{m}_{wf} \frac{(h_{pump,out,is} - h_{pump,in})}{\eta_{is,pump}\eta_{pump}} \quad 1$$

The total electricity savings are defined as the sum of the electricity generated by the ORC and the reduction in power consumption of the air dry coolers, relative to the total electrical power consumption of the base-case system, as expressed in Equation (9).

$$\%savings = \frac{P_{e,ORC} + P_{e,DC} - P_{e,DC,with\ ORC}}{P_{e,c} + P_{e,DC}} \times 100\% \quad (9)$$

The main modeling assumptions are summarized in Table 2. The expander is assumed to operate with an isentropic efficiency of 70% [24-26] and an electromechanical efficiency of 96% [27]. For the pump, isentropic compression is considered, along with a conservative overall efficiency of 65% to account for mechanical and motor losses [28-30]. A superheating degree of 10 K is imposed at the expander inlet, while a subcooling of 5 K at the ACC outlet is assumed to prevent cavitation [31]. The ACC operates with ambient air at 20 °C and a fan motor efficiency of 90%.

The ORC working fluid is isobutane. The working fluid mass flow rate and condensation temperature are determined to satisfy the specified pinch point temperature differences in the evaporator (10 K) and condenser (5 K), respectively [32]. Additionally, the cooling air flow rate is adjusted to achieve a temperature rise of 20 K across the ACC. An air-side pressure drop of 0.0015 bar is assumed [33]. Given the significance of this parameter, a parametric analysis is conducted to evaluate its impact on system performance.

Table 2. *ORC modeling assumptions*

Efficiencies	
Expander isentropic efficiency	70 % [24-26]
Pump global efficiency	65 % [28-30]
Electromechanical efficiency	96 % [27]
ACC fan motor efficiency	90%
Heat exchangers	
Ambient air temperature at ACC inlet	20°C
Temperature lift of air in ACC	10 K [34]
Pinch point in evaporator	10 K [31]
Pinch point in condenser	10 K [35]
Subcooling degree in condenser outlet	5 K [31]
Superheating degree at expander inlet	10 K [31]
Air pressure drop in ACC	0.0015 bar [33]
Pressures and temperatures	
Evaporator pressure	optimized
Condensation pressure (p_{cond})	calculated to satisfy pinch point in condenser

3. Results

3.1. Base case compression system

A parametric investigation varying the discharge pressure of both systems was conducted to identify the behavior of important system indicators. The optimization option was enabled for all simulations and the discharge pressure range is 300-500 bar for the four-stage system and 350-700 bar for the five-stage system. For the four-stage configuration, the maximum discharge pressure was limited to 500 bar, as higher pressures would result in compressor outlet temperatures exceeding the allowable threshold. For the five-stage configuration, discharge pressures lower than 350 bar were not considered, as the resulting pressure ratios

across the compression stages would fall significantly below the recommended operational range of 2–2.5. The investigated indicators are the compressor specific electric consumption, pressure ratio, intercooler heat duty and cooling water outlet temperature. Figures 4-7 exhibit those results for both systems.

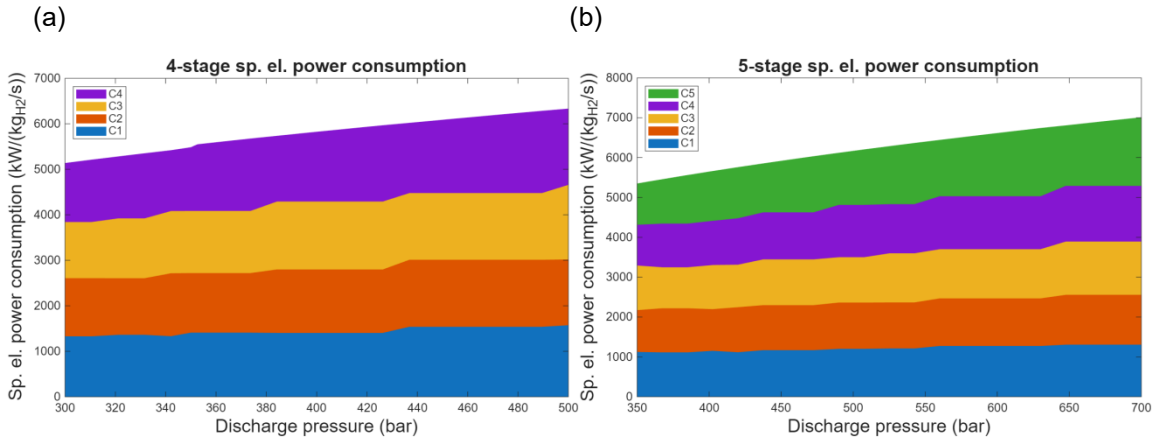

Figure 4. *Compressor specific electric power consumption a) for the four-stage system, and b) for the five-stage system*

There is an increase in power consumption for higher discharge pressures, however it can be observed as "steps" for every compression stage apart from the last one. In order to minimize the total compressor work for every system discharge pressure, the optimization solver has divided the complete range into sub-parts with increasing but constant pressure ratios (Figure 5) for all N-1 compressors, while linearly increasing the final pressure ratio for each step. In this way it ensures most efficient operation, even though it may not translate into a real system. All other variables illustrated in Figures 6-8 follow this operation.

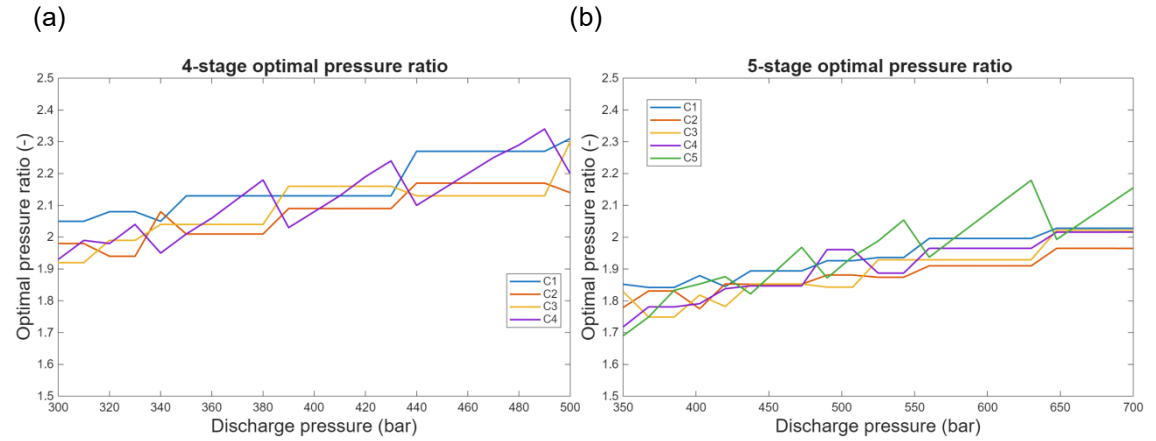

Figure 5. *Compressor optimal pressure ratio a) for the four-stage system, and b) for the five-stage system*

It is observed that for both systems the pressure ratio of all compressors increases for larger discharge pressures but remains in the range of 1.7-2.1, very close to the values calculated by Equation (1).

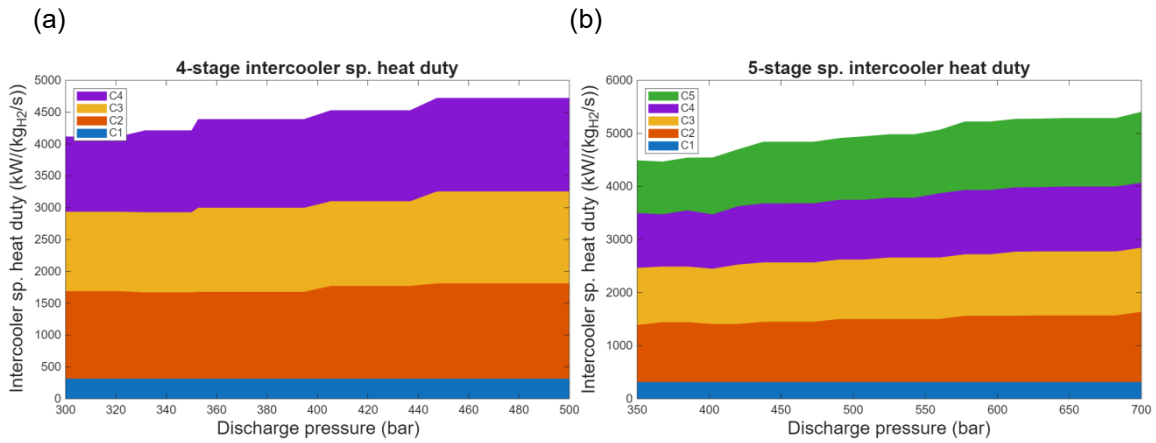

Figure 6: *Intercooler heat duty a) for the four-stage system, and b) for the five-stage system*

As the first intercooler corresponds to the initial cooling stage of hydrogen at the electrolyzer outlet, prior to compression, the hydrogen and cooling water temperatures remain unchanged across different discharge pressure scenarios. Consequently, the heat duty of this intercooler remains constant.

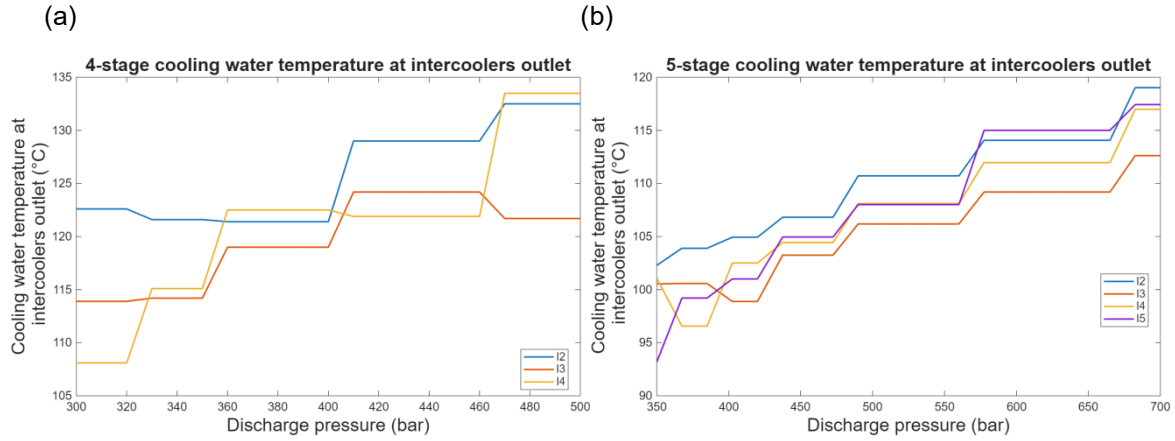

Figure 7. *Cooling water temperature after heat removal from the hydrogen in the intercoolers a) for the four-stage system, and b) for the five-stage system*

The cooling water temperature at the outlet of the first intercooler is consistently 50 °C across all discharge pressure cases, indicating insufficient thermal potential for effective utilization in the ORC. Consequently, this stream is excluded from the ORC analysis and is omitted from Figure 7.

The specific electric power consumption of the air dry coolers increases in steps in the range of 28.3-32.8 kW/kg_H_2 for the four-stage system and in the range of 31.2-37.5 kW/kg_H_2 for the five-stage system.

3.2. Waste heat recovery through ORC

The results concerning the electricity generated by the ORC system are presented in this section. Figure 8 shows the normalized power output of the ORC for both systems.

(a) (b)

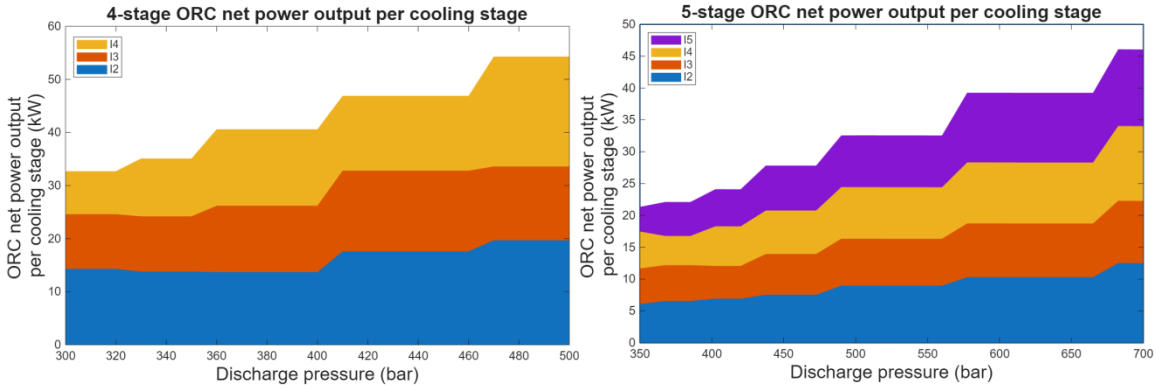

Figure 8. ORC normalized power output *a) for the four stage system, and b) for the five stage system*

It can be observed that the power generation for the four stage system is larger than the one for the five stage system, even though there are fewer heat sources. As can be seen in Figure 5, the pressure ratios for the five stage system are smaller, leading to lower hydrogen discharge temperatures. Subsequently the cooling water temperature at the intercoolers' outlets is also lower.

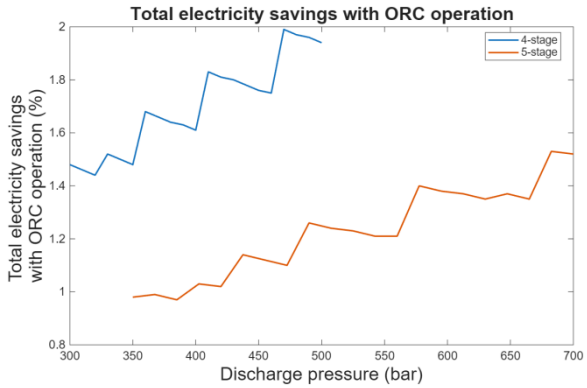

Figure 9. *Total electricity savings from ORC operation*

The total electricity savings (Figure (9)) are calculated by Equation (9).They are in the range of 1.4 – 2% for the 4 stage system and 0.98 – 1.5% for the 5 stage system. Those results align with the above indicators, since both the electricity generation as well as the dry cooler energy savings are lower for the 5 stage case. The saved electricity from the ORC operation ($P_{e,ORC} + P_{e,DC} - P_{e,DC,with\ ORC}$) linearly increases for higher discharge pressures, however the total electricity consumption of the base case ($P_{e,c} + P_{e,DC}$) increases in steps, due to the optimization tool operation. Therefore Equation (9) follows this zigzag form for both systems.

4. Conclusions

This study investigated the performance of multistage mechanical hydrogen compression systems for discharge pressures of 350 bar and 700 bar, coupled with a waste heat recovery configuration based on an Organic Rankine Cycle (ORC). The developed Aspen Plus model enabled the evaluation of compressor operation, interstage thermal behavior, and the potential for energy recovery through the utilization of intercooling heat.

The results indicate that increasing the discharge pressure leads to higher specific compression work, while the optimization of interstage pressure ratios ensures near-optimal operation within realistic constraints. The analysis also showed that the thermal potential of the intercoolers varies significantly across stages, with the first intercooler contributing negligible recoverable heat due to its low temperature level.

The integration of the ORC system demonstrated a measurable but very moderate improvement in overall system performance. Total electricity savings were found to range between approximately 1.4–2% for the four-stage configuration and 0.98–1.5% for the five-stage configuration. Despite the larger number of heat sources in the five-stage system, the lower temperature levels of the recovered heat resulted in reduced ORC performance compared to the four-stage case.

Overall, the study confirms that waste heat recovery from hydrogen compression systems is technically feasible and can contribute to a system efficiency improvement, although its effectiveness is strongly dependent on the temperature level of the available heat. The findings highlight the importance of thermodynamic matching between heat sources and recovery technologies.

Acknowledgments

This work has been performed in the context of the EXCELLEND project, which has received funding from the European Union's Horizon Europe research and innovation programme under grant agreement nr. 101185742. Views and opinions expressed here are those of the authors only and do not necessarily reflect those of the European Union or the European Research Executive Agency (REA). Neither the European Union nor the granting authority can be held responsible for them.

Nomenclature

h	specific enthalpy, (kJ/kg)
m	mass flow rate , (kg/s)
N	number of compression stages, (-)
P	power, (kW)
p	pressure, (bar)
Q	heat duty, (kW)
s	specific entropy, (kJ/kg·K)
T	temperature, (°C)
$\dot{V}$	volumetric flow rate, (m^3/s)

Greek symbols

η	efficiency

Subscripts and superscripts

ACC	air cooled condenser
DC	dry cooler
e	electric
em	electromechanical
ex	expander
is	isentropic
m	mechanical
ORC	organic Rankine cycle
wf	working fluid

References

[1] United Nations Environment Programme. Emissions gap report 2019. UNEP; 2019.

[2] International Energy Agency (IEA). Global hydrogen review 2023. Paris, France: International Energy Agency; 2023.

[3] Usman MR. Hydrogen storage methods: review and current status. Renew Sustain Energy Rev 2022;167.

[4] CoSMHyC Project. CoSMHyC – Co-electrolyser / methanation / hydrogen compressor hybrid conversion system – Available at: https://cosmhyc.eu/cosmhyc-project [accessed 23.3.2026].

[5] H2REF Project. H2REF – High performance electrolyser and refuelling system integration – Available at: https://h2ref.eu/ [accessed 23.3.2026].

[6] Fraunhofer UMSICHT. ELCHPEM – Compression hydrogen project – Available at: https://www.umsicht.fraunhofer.de/en/projects/elchpem-compression-hydrogen.html [accessed 23.3.2026].

[7] Zhang R, Cai J, Zhang T, Shi Z. Performance analysis and optimization of a TEG-based compression hydrogen storage waste heat recovery system. Renew Energy 2023;219(P2).

[8] U.S. Department of Energy (DOE), 2020, *Hydrogen Delivery Technical Team Roadmap*, U.S. Department of Energy, Washington, DC, USA.

[9] International Energy Agency (IEA), 2019, *The Future of Hydrogen*, International Energy Agency, Paris, France.

[10] International Organization for Standardization (ISO), 2018, *ISO 19881: Gaseous hydrogen — Land vehicle fuel tanks*, ISO, Geneva, Switzerland.

[11] American Petroleum Institute (API). Reciprocating compressors for petroleum, chemical, and gas industry services (API Standard 618). Washington, DC, USA: American Petroleum Institute; 2013.

[12] Braimakis K. Mapping the waste heat recovery potential of CO_2 intercooling compression via ORC. Int J Refrig 2024;159:309-32.

[13] Khan MA, Young C, Mackinnon C, Layzell DB. The techno-economics of hydrogen compression. Transition Accelerator Technical Briefs 2021;1(1):1-36.

[14] Mokhatab S, Poe WA, Mak JY. Handbook of natural gas transmission and processing: principles and practices. Gulf Professional Publishing; 2018. p. 444-58.

[15] Aijun, C., Jun, P., Hang, Z., et al., 2025, Experimental investigation of hydrogen production performance of PEM electrolyze, *Scientific Reports*, 15: 23230.

[16] Wang, C.R., Stansberry, J.M., Mukundan, R., et al., 2025, Proton exchange membrane (PEM) water electrolysis: Cell-level considerations for gigawatt-scale deployment, *Chemical Reviews*, 125(3): 1257–1302.

[17] AspenTech. Aspen Plus V14 – Aspen One process simulation for energy and chemicals; 2024.

[18] International Renewable Energy Agency (IRENA). Green hydrogen cost reduction: scaling up electrolysers to meet the 1.5°C climate goal. Abu Dhabi, UAE: International Renewable Energy Agency; 2020.

[19] Aspen Technology Inc., 2011, Aspen One V7: Process Optimization for Engineering Manufacturing and Supply Chain, Aspen Technology, Burlington, ON, Canada.

[20] Farajollahi, H., Hossainpour, S., 2017, Application of organic Rankine cycle in integration of thermal power plant with post-combustion CO2 capture and compression, *Energy*, 118: 927–936.

[21] Braimakis, K., Grispos, V., Karellas, S., 2021, Exergetic efficiency potential of double-stage ORCs with zeotropic mixtures of natural hydrocarbons and CO2, *Energy*, 218: 119577.

[22] Braimakis, K., et al., 2020, Exergetic performance of CO2 and ultra-low GWP refrigerant mixtures as working fluids in ORC for waste heat recovery, *Energy*, 203: 117801.

[23] Braimakis, K., et al., 2015, Low grade waste heat recovery with subcritical and supercritical Organic Rankine Cycle based on natural refrigerants and their binary mixtures, *Energy*, 88: 80–92.

[24] Astolfi, M., 2015, Techno-economic optimization of low temperature CSP systems based on ORC with screw expanders, *Energy Procedia*, 69: 1100–1112.

[25] Scagnolatto, G., Cabezas-Gómez, L., Bigonha Tibiriçá, C., 2021, Analytical model for thermal efficiency of organic Rankine cycles, considering superheating, heat recovery, pump and expander efficiencies, *Energy Conversion and Management*, 246: 114628.

[26] Quoilin, S., et al., 2011, Thermo-economic optimization of waste heat recovery organic Rankine cycles, *Applied Thermal Engineering*, 31(14): 2885–2893.

[27] McCoy, G.A., Douglass, J.G., 2014, *Premium efficiency motor selection and application guide—A handbook for industry*, US Department of Energy, Washington, DC, USA.

[28] Li, D., et al., 2021, Thermodynamic analysis and optimization of a partial evaporating dual-pressure organic Rankine cycle system for low-grade heat recovery, *Applied Thermal Engineering*, 185: 116363.

[29] Xu, W., et al., 2017, Novel experimental research on the compression process in organic Rankine cycle (ORC), *Energy Conversion and Management*, 137: 1–11.

[30] Li, Z., et al., 2019, Analysis of a combined trilateral cycle - organic Rankine cycle (TLC-ORC) system for waste heat recovery, *Energy Procedia*, 158: 1786–1791.

[31] Maraver, D., et al., 2014, Systematic optimization of subcritical and transcritical organic Rankine cycles (ORCs) constrained by technical parameters in multiple applications, *Applied Energy*, 117: 11–29.

[32] Braimakis, K., Karellas, S., 2017, Integrated thermoeconomic optimization of standard and regenerative ORC for different heat source types and capacities, *Energy*, 121: 570–598.

[33] Lecompte, S., et al., 2013, Part load based thermo-economic optimization of the Organic Rankine Cycle (ORC) applied to a combined heat and power (CHP) system, *Applied Energy*, 111: 871–881.

[34] Sohrabi, A., Behbahaninia, A., Sayadi, S., 2021, Thermodynamic optimization and comparative economic analysis of four organic Rankine cycle configurations with a zeotropic mixture, *Energy Conversion and Management*, 250: 114872.
[35] Zhou, Y., Zhang, F., Yu, L., 2016, Performance analysis of the partial evaporating organic Rankine cycle (PEORC) using zeotropic mixtures, *Energy Conversion and Management*, 129: 89–99.